TAGUCHI METHOD APPLICATION FOR EXTERNAL AIRFOIL FLAPS OPTIMIZATION

Y Anupam Rao[1*], Subhash Gautam[2], Aneesh Somwanshi[3], Milan Choubey[4]

Article History: Received: 26.04.2023 **Revised:** 11.06.2023 **Accepted:** 21.07.2023

Abstract

The Taguchi optimization of an external airfoil flap was performed numerically in the current study. ANSYS-Fluent software was used for two-dimensional analyses. Six different turbulence models were used for experimental validation, and the Spalart-Allmaras turbulence model was found to be the most precise. The study found that when the angle of attack is 10°, the NACA 4412 airfoil should be used for both external and base airfoils to maximise aerodynamic performance. Furthermore, the CL/CD ratio was maximised when the external airfoil angle was equal to 10° and length of external airfoil was 0.15*chord length. While the maximum CL/CD ratio for NACA 0018 was found to be 31,36 and 42,54 for NACA 4412, it was calculated 44,69 for the optimised design.

Keywords: Airfoil, External Flap, Taguchi, Aerodynamic, Wind Energy.

[1*]Assistant Professor, Department of Mechanical Engineering, Oriental Institute of Science and Technology, Jabalpur, Madhya Pradesh, India
Email: [1*]anupamrao@oriental.ac.in
[2]Assistant Professor, Department of Mechanical Engineering, College of Agriculture Engineering, JNKVV Jabalpur, Madhya Pradesh, India
[3]Associate Professor, Department of Mechanical Engineering, MATS University, Raipur, Chhattisgarh, India
[4]PhD Scholar, UTD SoEEM, Rajiv Gandhi Proudyogiki Vishwavidyalaya, Bhopal, Madhya Pradesh, India

[*]Corresponding Author:
Y Anupam Rao[1*]
[1*]Assistant Professor, Department of Mechanical Engineering, Oriental Institute of Science and Technology, Jabalpur, Madhya Pradesh, India
Email: [1*]anupamrao@oriental.ac.in

DOI: 10.31838/ecb/2023.12.s3.730

1. Introduction

A wing is a critical component of a wind turbine, plane, or aircraft. The two main types of forces that are usually attributed to an airfoil are lift and drag forces, which are created as the flow passes over the airfoil [1]. The drag force is parallel to the flow path, while the lift force is perpendicular to the wind direction. Airfoil optimization is critical for a wind turbine or aircraft wing. Because airfoil-shaped cross sections are commonly used in wind turbines, aircraft, and planes, the aerodynamic performance of airfoil shapes has a direct impact on the performance of a wing or a wind turbine. Many studies have been conducted to investigate the performance of airfoils or their impact on wind turbines. Ali et al. investigated the aerodynamic parameters of the NACA 6415 airfoil numerically. They discovered that when the angle of attack was equal to 10°, the maximum lift coefficient was observed. They also stated that the drag force increases as the angle of attack climbs [1]. Mousavi et al. created a simulation of a subsonic turbulent flow over the NACA 0012 airfoil. They found out that the Spalart-Allmaras turbulence model has the highest accuracy [2] as a result of their research. Song et al. used a machine learning-based algorithm to optimise a NACA 0012 airfoil [3]. Ayaz Ümütlü and Kral optimised a NACA 4415 airfoil using the Bézier curve and a genetic algorithm [4].Abobaker et al. investigated the effect of mesh type on an airfoil's aerodynamic coefficients [5].Loutun et al. compared the aerodynamic performance of various airfoils for a Vertical Axis Wind Turbine. They stated that while NACA 0018 has the best aerodynamic performance for a wind turbine, NACA 0010 has the worst [6]. The aerodynamic feature of the NACA 0018 airfoil for a Darrieus wind turbine were numerically studied by Rogowski et al. [7].Kruse et al. investigated various types of leading edge roughness in a NACA 633-418 airfoil [8]. Butt et al. studied the flow over NACA 0021 and NACA 4412 airfoils, which are commonly used for wind turbine blades. They compared the lift and drag forces on airfoils with and without tubercles [9]. Lewthwaite and Amaechi investigated the winglet aerodynamics and dimple effect of the NACA 0017 airfoil numerically [10].Genç et al. studied pre-stall flow control on the NACA 4412 wind turbine blade airfoil [11]. The effect of thickness and camber ratio on flow characteristics over various airfoils was investigated by Karasu et al. [12]. The role of the laminar separation bubble in flow evolution and flow over the NACA 4412 airfoil was investigated by Koca et al. [13].Sahin and Acr investigated the aerodynamic coefficients of the NACA 0015 wind turbine airfoil numerically and experimentally [14].

The Taguchi optimization was used in this study to improve the aerodynamic performance of an airfoil with an external flap. ANSYS-Fluent software was used for numerical analyses. The One-Way Analysis of Variance was used to determine the contribution of each parameter. The aerodynamic performance of selected airfoils was determined using the lift coefficient to drag coefficient ratio.

2. Material and method

Basic Formulations

The Reynolds number (Re) is calculated with the following equation;

$$Re = \frac{\rho U c}{\mu}$$

In this equation, ρ is the fluid density, U is the flow speed, c is the chord lengthand μ is the dynamic viscosity.

In order to determine the aerodynamic performance of airfoils, lift and drag forces should be calculated. Coefficient of Lift (C_L) and Coefficient of Drag (C_D) defined as [4];

$$C_L = \frac{2F_L}{\rho U^2 S}$$
$$C_L = \frac{2F_D}{\rho U^2 S}$$

C_L and C_D were calculated using Reynolds Averaged Navier-Stokes (RANS) equations. The Conservation of mass and momentum can be given as [4];

Conservation of mass, $\nabla . \underline{u} = 0$.Conservation of momentum, $\rho \frac{D\underline{u}}{Dt} = -\nabla p + \mu \nabla^2 u + \rho \underline{F}$

In these equations, $\underline{u}$ is the velocity vector, $= -\nabla p + \mu \nabla^2 u$ shows the internal forces and $\rho \underline{F}$ is the external forces.

For NACA airfoils, the first digit displays the chord length's maximum curvature as a percentage. The second digit represents the camber position and final two digits display the chord length to blade thickness ratio [15]. In Figure 1, airfoil aerodynamic parameters were shown along with C_L and C_D Values vs. the Number of Mesh Elements

Geometric domain and mesh generation

Mesh independence tests were carried out in order to accomplish the most reasonable results in the shortest amount of time.Furthermore, the computational domain size was optimized. CL and CD were calculated at a 10° angle of attack using six different mesh structures. Figure 1 depicts the change in CL and CD values as the number of mesh elements increases. The difference between the calculated CL and CD values for the number of mesh elements = 197067 and 250209 is less than 1%. As a result, the mesh structure with 197037 mesh elements was used for the following stages of this study.The selected mesh point is represented by the black circle.

The mesh structure plays a very important role in terms of the needed solution time. If the mesh structure is created in a very detailed way, solution takes longer. If the number of mesh elements is too low, results will not be reasonable. This is also true for the computational domain size. If the computational domain is generated too wide, the number of mesh elements will be increased also, and the solution time will be increased. If the domain is too small, observed results will be wrong. Figure 2 shows the created computational domain. In this Figure, A, B and C show the domain sizes. Inlet, outlet and symmetry boundary conditions were applied on edges.

C_L and C_D values for different sizes of A, B and C were calculated at an angle of attack of 10°. The sizes of A, B and C were changed and it was aimed to create the smallest computational domain while keeping the solution reliability. Figure 3 shows the change in C_L and C_D values versus the sizes of A, B and C.

C_L values were calculated as 0,901, 0,9 and 0,899 for the size of A = 20c, 30c and 40c, respectively. Also, C_D values were detected as 0,02804, 0,02817 and 0,0284 for the size of A = 20c, 30c and 40c, respectively. Since differences between C_L and C_D values were small, the size of A was selected as 20c. Same calculations were also conducted in order to determine the optimum sizes of B and C. It was seen that when the size of B is equal to 10c, 15c and 20c, C_L and C_D values were changed significantly. So, the length of B was selected as 10c. When the size of C is equal to 10c, 20c and 40c, C_L values were calculated as 0,893, 0,899 and 0,898 respectively. C_D values were determined as 0,0295 for C = 10c, 0,0286 for C = 20c and 40c. The difference between observed C_L values was quite low. However, when C = 10c and 20c, the difference between calculated C_D values is approximately 3%. Therefore, the length of C was selected as equal to 20c since C_L and C_D werecalculated approximately the same for C = 20c and 40c.

Turbulence Model and Numerical Settings

Six different turbulence models that are Spalart-Allmaras, Realizable $k-\varepsilon$, Renormalization Group (RNG) $k-\varepsilon$, Standard $k-\varepsilon$, k–omega $(k-\omega)$ and Shear stress transport k–omega $(SST\ k-\omega)$ were tested in order to validate experimental results[16]for the NACA 0018 airfoil at Re = 300000.

It was seen from Figure 4 that the Spalart-Allmaras turbulence model gives the closest results to experimental values, for both C_L and C_D. So, for the next steps, the Spalart-Allmaras turbulence model was used. The Spalart-Allmaras turbulence model was created specifically for aerospace applications that involve space or aero body parameters, such as airfoil [17]. Wind speed was set to 42,5 m/s and the cord length of the modelled airfoil is 0,1 m. To solve the momentum and turbulent viscosity, the second order upwind formulation was used.

Method of Taguchi

The method of Taguchi is a useful optimization method in order to reduce the needed number of experiments and find the optimum solution. This method can be used for both industrial and academic applications. To determine the process quality, it uses the Signal-to-Noise (S/N) ratio. There are three different ways to calculate the S/N ratio;

Smaller is better;

$$S/N = -10log\frac{1}{n}\left(\sum y^2\right)$$

Larger is better;

$$S/N = -10log\frac{1}{n}\left(\sum \frac{1}{y^2}\right)$$

Nominal is better;

$$S/N = 10log\frac{\vec{y}}{s_y^2}$$

Since the aim of this study is to increase the C_L/C_D ratio, the larger is better equation was used.

Degrees of Freedom (DOF) must be considered while selecting the orthogonal array that shows th Base Airfoil needed experiments. For an orthogonal array, DOF is equal to the total number of experiments – 1. For a selected parameter, DOF = the number of levels – 1. The total number of DOF for an orthogonal array has to be greater or equal to the total number of DOF for selected parameters [18]. Table 1 shows selected parameters and their levels in order to increase the C_L/C_D ratio. Figure 5 shows the created design.

There are five different parameters that are base airfoil cross section, external airfoil cross section, distance between the external and the base airfoil, external airfoil length and external airfoil anglewere selected in order to climb the C_L/C_D ratio. Five different levels were chosen for each parameter. Normally, to find the optimum combination of selected parameters for maximizing the C_L/C_D ratio, 5^5 = 3125 numerical analyses have to be conducted. In this study, for selected parameters, DOF = 5 (number of parameters) * (5-1) = 20. So, the L_{25} orthogonal design was selected. By this way, it was aimed to find the optimum combination with only 25 numerical analyses rather than 3125 numerical analyses.

3. Results

As mentioned before, since the DOF of selected parameters is equal to 20, the L_{25} orthogonal array was created by using Minitab software. In Table 2, the created orthogonal array, calculated C_L/C_D ratios and S/N ratios were shown. The angle of attack (α) was set to 10°, where the maximum C_L/C_D was observed between 2° $<(\alpha)<$ 18° (see in Figure 4). ANSYS Fluent software was used to calculate C_L/C_D ratiosand S/N ratios were determined with Minitab software by using theLarger is Better formulation. While determining S/N ratios, C_L/C_D ratios were used. As seen in Table 2, the maximum C_L/C_D ratio was calculated with the 20th analysis as 38,158, with the A4B5C3D1E4 design. The A4B5C3D1E4 design indicates that the base airfoil is NACA 4412, the external airfoil is NACA 4418, the distance between the base airfoil and the external airfoil is equal to 0,1c, the external airfoil length is 0,05c and the external airfoil angle is 15°.

With calculated S/N ratios, the main effects plot for S/N ratios graph was created. Figure 6 shows the S/N ratios for different parameters and levels. As the Larger is Better formulation was used, the bigger S/N ratio means the higher C_L/C_D ratio.

It can be seen that for the parameter A (Base airfoil cross section), level 4 (NACA 4412) should be used to maximize C_L/C_D (see in Table 1). So, B, C, D and E should be level 4, level 1, level 3 and level 3, respectively. It means to achieve the highest C_L/C_D ratio, the A4B4C1D3E3 combination should be used. Table 3 shows the response table for calculated S/N ratios. Here, delta is the difference between the calculated maximum and minimum S/N ratios for a parameter and Rank shows the parameter's effect. From Table 3, it can be seen that the parameter A affects the C_L/C_D ratio the most and the parameter E affects it the least.

It is possible to estimate the maximum C_L/C_D ratio, which should be observed with the A4B4C1D1E3 combination with the following equation [19];

$$\eta_{mean} + \Delta A4 + \Delta B4 + \Delta C1 + \Delta D3 + \Delta E3 = -10\log_{10}\left(\frac{1}{C_L/C_D{}^2}\right)$$

Here, η_{mean} is the overall S/N ratios for 25 different analyses (see in Table 2) and $\Delta A4$ shows the difference between the overall S/N ratio and the S/N ratio for A4 (29,77, see in Table 3). So, the maximum C_L/C_D ratio for the A4B4C1D3E3 combination can be calculated as;

$$29 + 0{,}77 + 0{,}62 + 0{,}75 + 0{,}42 + 0{,}47 = -10\log_{10}\left(\frac{1}{{C_L/C_D}^2}\right), C_L/C_D = 39{,}95$$

The Analysis of Variance (ANOVA) analysis was conducted to find each parameter's contribution to the C_L/C_D ratio. Table 4 shows the ANOVA analysis. Here, MS is the means of square, the higher MS is the higher the impact and MS=SS/DOF. SS is the sum of squares. So, in this table, it can be seen that the base airfoil cross section contributes to the C_L/C_D ratio by 46,63%. Furthermore, B (external airfoil cross section), C (distance between airfoil and external airfoil), D (external airfoil length) and E (external airfoil angle) contribute to $C_L/C_D$by 14,55%, 18,35%, 4,51% and 8,25%, respectively.

In the next step, the A4B4C1D3E3 design was created and C_L, C_D and C_L/C_D ratios were observed. Moreover, the aerodynamic characteristic of the optimum design was compared with the NACA 0018 and NACA 4412 airfoil performance. Figure 7 shows C_L and C_D values of the optimum design, NACA 0018 and NACA 4412 airfoil.

As seen in Figure 7, C_L values of the A4B4C1D3E3 design are bigger than C_L values of other two airfoil cross sections when the α is bigger than 4°.The stall angle remained the same. The maximum C_L was calculated as 1,6458 for the optimum design, 1,1094 for the NACA 0018 and 1,4744 for the NACA 4412 at α = 14°. However, the C_D was also increased by using the A4B4C1D3E3 design, especially at higher α values. Figure 8 shows the C_L/C_D ratios of the optimum design, NACA 0018 and NACA 4412 airfoil.

As seen in Figure 8 , When α is bigger than 12°, higher C_L/C_D values were detected with NACA 0018 and NACA 4412 airfoils than the optimum design. The optimum design showed better performancethan other airfoils at 4° <α< 12°. While the maximum C_L/C_D was determined as 44,69 for the optimum design at α = 8°, it was determined as 31,36 for NACA 0018 at α = 10° and 42,54 for NACA 4412 at α = 6°. So, between 4° <α< 12°, it can be said that optimized design has more aerodynamic performance than other airfoil cross sections. Furthermore, as mentioned before, the maximum C_L/C_Dat α = 8° was estimated as 39,95 by using calculated S/N ratios for the optimized design. With numerical analysis, it was calculated as 41,44. So, the difference between calculated and numerically performed C_L/C_Dvalues is only 3,73%. This shows there is a good agreement between estimated and numerically performed C_L/C_Dvalues.

4. Conclusions

In this study, the effect of an external flap on the aerodynamic performance of an airfoil was investigated numerically in two-dimensions using ANSYS - Fluent software. To increase the C_L/C_D ratio, the Taguchi optimization method was used. Five different parameters, which are the base airfoil cross section, external airfoil cross section, distance between the external and the base airfoil, external airfoil length and external airfoil angle were selected for the optimization process.

- Numerical results showed that the Spalart-Allmaras turbulence model gives the closest results to experimental values.
- To decrease the needed number of mesh elements and the solution time, computational domain sizes were optimized. So, it was seen that the inlet and both symmetry sides should be at least 10c away from the airfoil. Furthermore, the distance between the airfoil and the outlet side should be greater than 20c.
- L_{25} orthogonal design was created. At α = 10°, C_L/C_D values and S/N ratios were calculated. Using the calculated S/N ratios, the optimum combination for maximizing the CL/CD was found as A4B4C1D3E3 (Base airfoil cross section = NACA 4412, external airfoil cross section is NACA 4412, distance between base airfoil and external airfoil is 0, external airfoil length is 0,15 c and external airfoil angle is 10°).
- ANOVA analyses were performed. It was seen that the most important parameter

that effects the aerodynamic performance is the base airfoil cross section and the least important parameter is the external airfoil length.

- C_L, C_D and C_L/C_D ratios were calculated for the optimum design. Between $4° < \alpha < 12°$, A4B4C1D3E3 design showed better aerodynamic performance than the NACA 0018 and NACA 4412 airfoils.
- Maximum C_L/C_D ratios were found as 44,69 for the A4B4C1D3E3 design, 31,36 for NACA 0018 and 42,54 for NACA 4412.
- The maximum C_L/C_D ratio for the optimum design at $\alpha = 10°$ was found as 39,95 using the S/N ratios and 41,44 with numerical analysis.
- For future studies, different flap types can be investigated. Furthermore, different dimple and flap types can be used at the same time.

5. References

1. Ali R, Akhtar S, Farhan M, Alam F. Numerical investigation of aerodynamic parameters across NaCa6415 airfoil. Mater Today Proc 2021;45:3047–53. https://doi.org/10.1016/j.matpr.2020.12.059.
2. MOUSAVI SM, AMINIAN J, SHAFIEI N, DADVAND A. NUMERICAL SIMULATION OF SUBSONIC TURBULENT FLOW OVER NACA0012 AIRFOIL: EVALUATION OF TURBULENCE MODELS. Sigma J Eng Nat Sci 2017;35:133–55.
3. Song X, Wang L, Luo X. Airfoil optimization using a machine learning-based optimization algorithm. J Phys Conf Ser 2022;2217. https://doi.org/10.1088/1742-6596/2217/1/012009.
4. Ayaz ümütlü HC, Kiral Z. Airfoil Shape Optimization Using Bézier Curve and Genetic Algorithm. Aviation 2022;26:32–40. https://doi.org/10.3846/aviation.2022.16471.
5. Abobaker M, Addeep S, Afolabi LO, Elfaghi AM. Effect of Mesh Type on Numerical Computation of Aerodynamic Coefficients of NACA 0012 Airfoil. J Adv Res Fluid Mech Therm Sci 2021;87:31–9. https://doi.org/10.37934/arfmts.87.3.3139.
6. Loutun MJT, Didane DH, Batcha MFM, Abdullah K, Ali MFM, Mohammed AN, et al. 2D Cfd Simulation Study on the Performance of Various Naca Airfoils. CFD Lett 2021;13:38–50. https://doi.org/10.37934/cfdl.13.4.3850.
7. Rogowski K, Kr G, Bangga G. Numerical Study on the Aerodynamic Characteristics of the NACA 0018 Airfoil at Low Reynolds Number for Darrieus Wind Turbines Using the Transition SST Model. Processes 2021;9.
8. Krog Kruse E, Bak C, Olsen AS. Wind tunnel experiments on a NACA 633-418 airfoil with different types of leading edge roughness. Wind Energy 2021;24:1263–74. https://doi.org/10.1002/we.2630.
9. Butt U, Hussain S, Schacht S, Ritschel U. Experimental investigations of flow over NACA airfoils 0021 and 4412 of wind turbine blades with and without Tubercles. Wind Eng 2022;46:89–101. https://doi.org/10.1177/0309524X211007178.
10. Lewthwaite MT, Amaechi CV. Numerical Investigation of Winglet Aerodynamics and Dimple Effect of NACA 0017 Airfoil for a Freight Aircraft. Inventions 2022;7. https://doi.org/10.3390/inventions7010031.
11. Serdar GENÇ M, KOCA K, AÇIKEL HH. Investigation of pre-stall flow control on wind turbine blade airfoil using roughness element. Energy 2019;176:320–34. https://doi.org/10.1016/j.energy.2019.03.179.
12. Karasu I, Açikel HH, Koca K, Genç MS. Effects of thickness and camber ratio on flow characteristics over airfoils. J Therm Eng 2020;6:242–52. https://doi.org/10.18186/THERMAL.710967.
13. Koca K, Genç MS, Açıkel HH, Çağdaş M, Bodur TM. Identification of flow phenomena over NACA 4412 wind turbine airfoil at low Reynolds numbers and role of laminar separation bubble on flow evolution. Energy 2018;144:750–64. https://doi.org/10.1016/j.energy.2017.12.045.
14. Şahin İ, Acir A. Numerical and Experimental Investigations of Lift and Drag Performances of NACA 0015 Wind Turbine Airfoil. Int J Mater Mech Manuf

2015;3:22–5. https://doi.org/10.7763/ijmmm.2015.v3.159.
15. Kaya AF, Acır A, Tanürün HE. Numerical investigation of radius dependent solidity effect on H-type vertical axis wind turbines. J Polytech 2020;0900:0–2. https://doi.org/10.2339/politeknik.799767.
16. Timmer WA. Two-dimensional low-Reynolds number wind tunnel results for airfoil NACA 0018. Wind Eng 2008;32:525–37. https://doi.org/10.1260/030952408787548848.
17. Shukla V, Kaviti AK. Performance evaluation of profile modifications on straight-bladed vertical axis wind turbine by energy and Spalart Allmaras models. Energy 2017;126:766–95. https://doi.org/10.1016/j.energy.2017.03.071.
18. Radune M, Lugovskoy S, Knop Y, Yankelevitch A. Use of Taguchi method for high energy ball milling of CaCO3. Int J Mech Mater Eng 2022;17:1–9. https://doi.org/10.1186/s40712-021-00140-8.
19. Karthikeyan P, Muthukumar M, Shanmugam SV, Kumar PP, Murali S, Kumar APS. Optimization of operating and design parameters on proton exchange membrane fuel cell by using Taguchi method. Procedia Eng 2013;64:409–18. https://doi.org/10.1016/j.proeng.2013.09.114.

Table 1. Selected Parameters and Levels

Parameters	***Level 1***	***Level 2***	***Level 3***	***Level 4***	***Level 5***
A, Base airfoil cross section	NACA 0012	NACA 0018	NACA 0024	NACA 4412	NACA 4418
B, External airfoil cross section	NACA 0012	NACA 0018	NACA 0024	NACA 4412	NACA 4418
C, Distance between base and external airfoil (s)	0	0,05c	0,1c	0,15c	0,2c
D, External airfoil length (c_e)	0,05c	0,1c	0,15c	0,2c	0,25c
E, External airfoil angle (β)	0°	5°	10°	15°	20°

Table 2.S/N ratios and C_L/C_D values for L_{25} orthogonal array.

Exp. No	***A***	***B***	***C***	***D***	***E***	***Cl/CD***	***S/N (dB)***
1	1	1	1	1	1	33,31	30,45149
2	1	2	2	2	2	31,37	29,93029
3	1	3	3	3	3	31,71	30,02392
4	1	4	4	4	4	33,73	30,56033
5	1	5	5	5	5	26,79	28,55945
6	2	1	2	3	4	24,88	27,91701
7	2	2	3	4	5	16,544	24,37281
8	2	3	4	5	1	19,7	25,88932
9	2	4	5	1	2	30,093	29,56931
10	2	5	1	2	3	35,92	31,10673
11	3	1	3	5	2	23,295	27,34525
12	3	2	4	1	3	21,1939	26,52422
13	3	3	5	2	4	16,83	24,52168
14	3	4	1	3	5	32,8965	30,34299
15	3	5	2	4	1	20,43	26,20537
16	4	1	4	2	5	28,6	29,12732
17	4	2	5	3	1	33,007	30,37212
18	4	3	1	4	2	36,33	31,20531
19	4	4	2	5	3	38,158	31,63171
20	4	5	3	1	4	38,263	31,65558
21	5	1	5	4	3	30,431	29,66632

22	5	2	1	5	4	33,304	30,44993
23	5	3	2	1	5	27,44	28,76768
24	5	4	3	2	1	29,177	29,30081
25	5	5	4	3	2	29,2	29,30766

Table 3. Response table for S/N ratios

Level	***A***	***B***	***C***	***D***	***E***
1	29,51	29,21	29,75	29,35	29,06
2	28,84	29,01	29,2	29,16	29,38
3	28,6	28,93	29,07	29,42	29,47
4	29,77	29,62	29,01	29,03	29,22
5	29,39	29,34	29,08	29,16	28,99
Delta	1,16	0,69	0,73	0,39	0,47
Rank	1	3	2	5	4

Table 4. ANOVA for the L_{25} design.

Parameter	***DOF***	***SS***	***MS***	***Contribution***	***F***	***P***
A	4	49,303	12,326	46,63%	6,06	0,055
B	4	15,388	3,847	14,55%	1,89	0,276
C	4	19,408	4,852	18,35%	2,38	0,21
D	4	4,776	1,194	4,51%	0,59	0,691
E	4	8,718	2,179	8,25%	1,07	0,474
Error	4	8,14	2,035	7,70%		
Total	24	105,733				

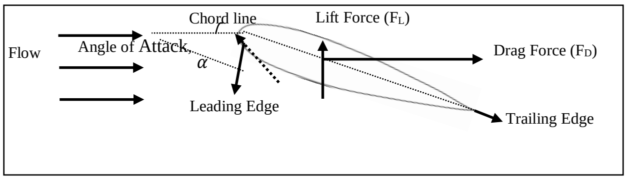

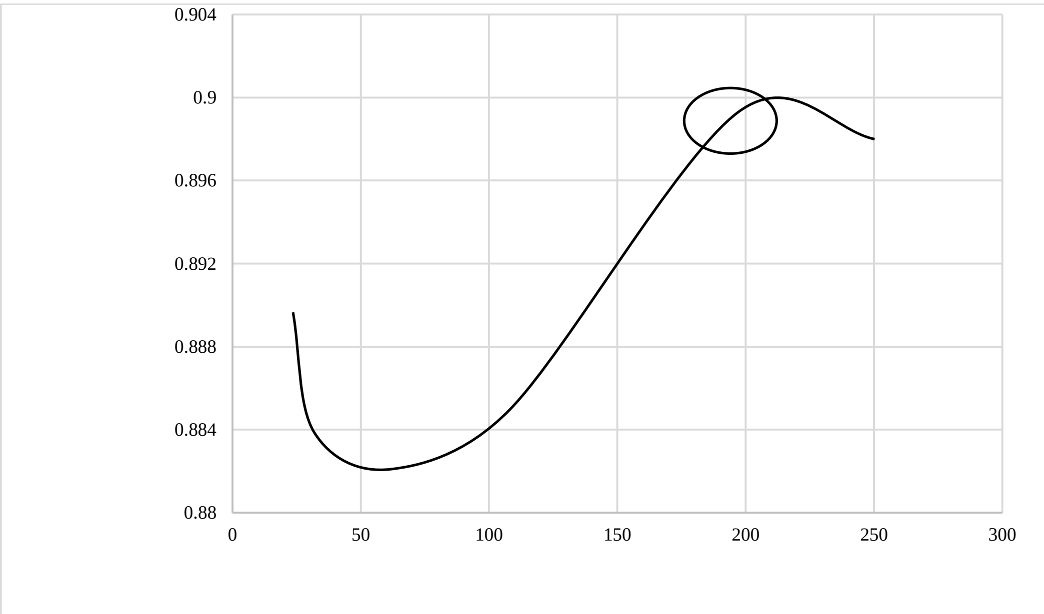

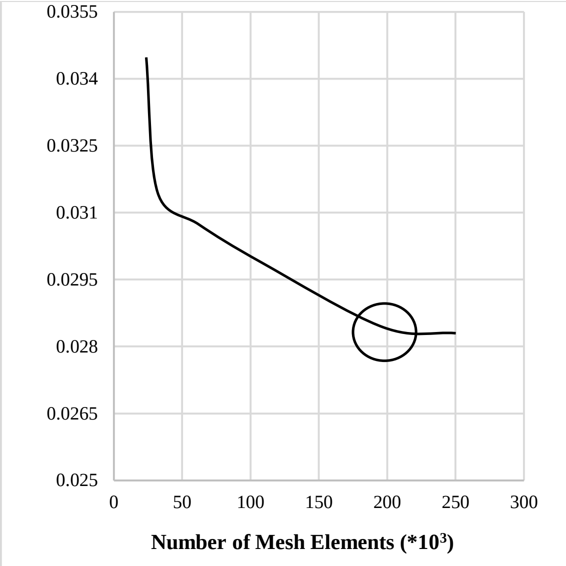

Figure 1. C_L and C_D Values vs. the Number of Mesh Elements

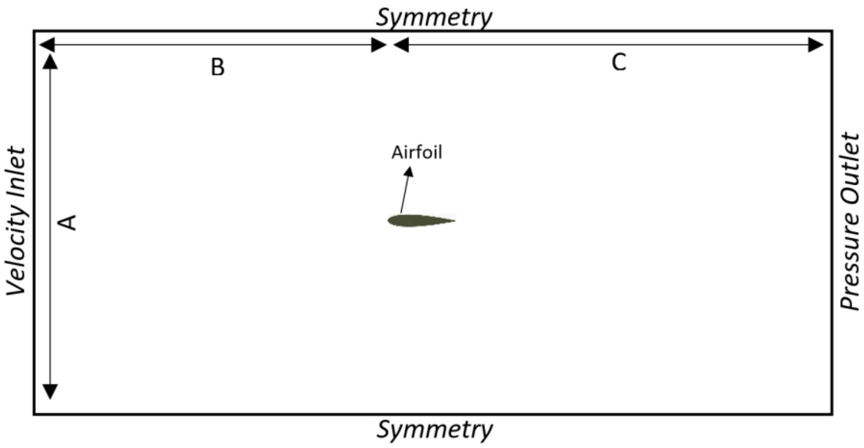

Figure 2. Computational Domain

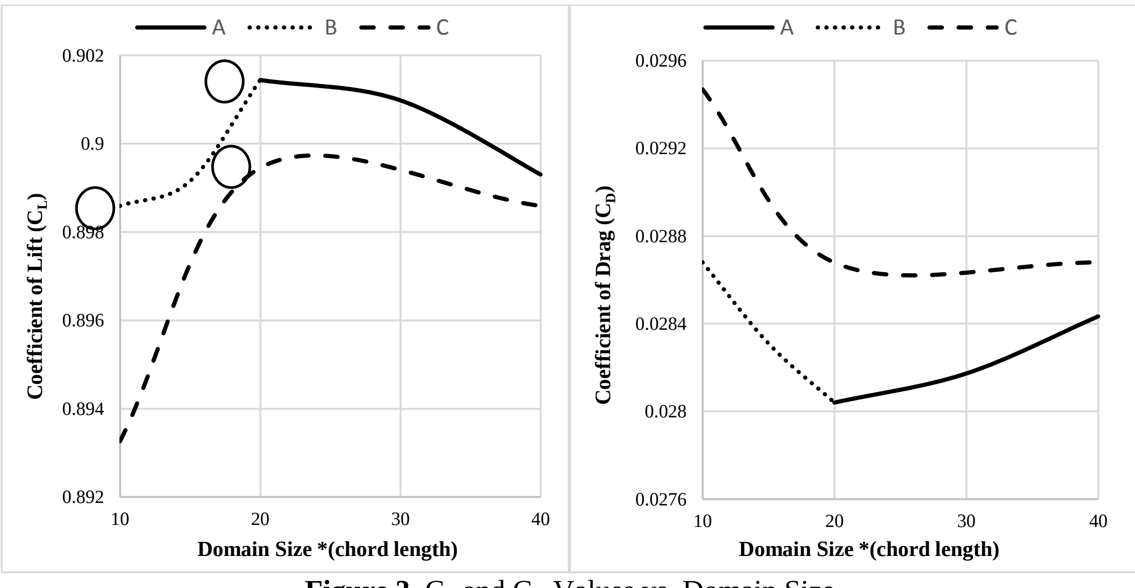

Figure 3. C_L and C_D Values vs. Domain Size

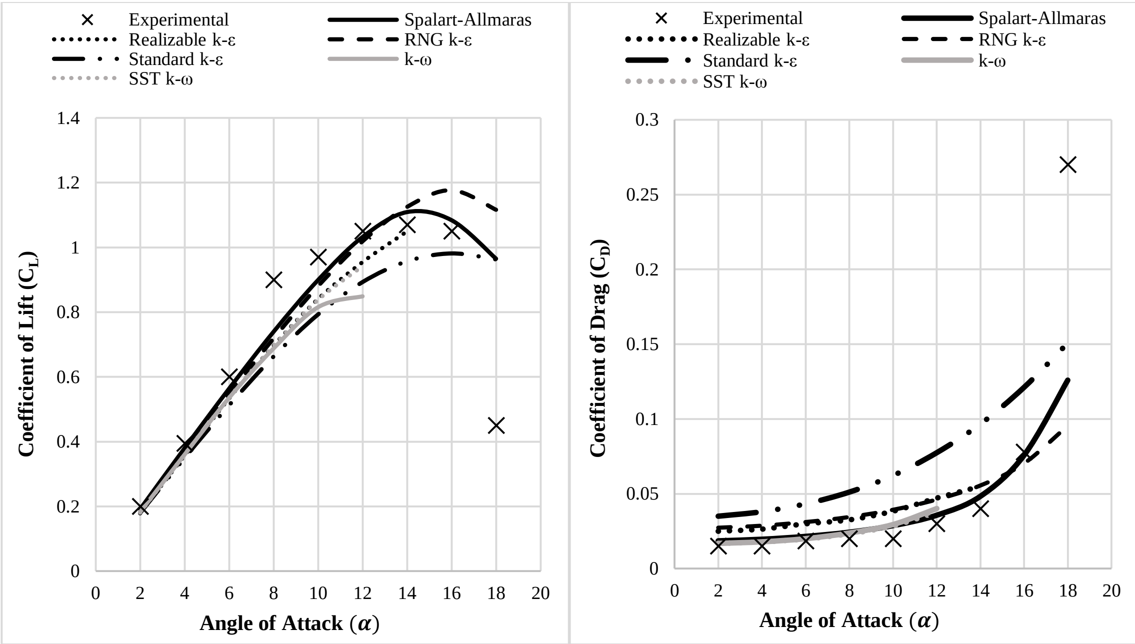

Figure 4. Validation Study

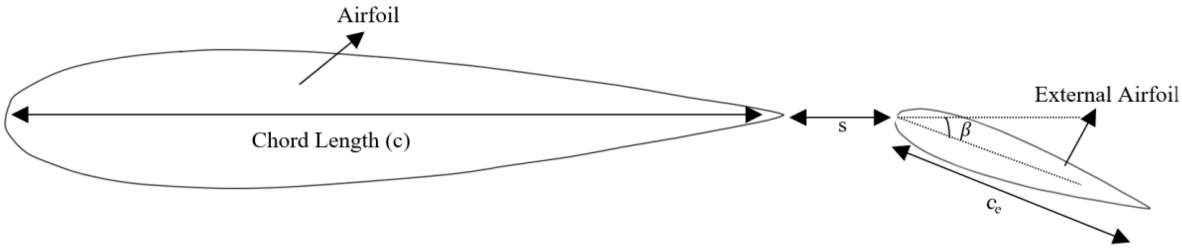

Figure 5. Created Design

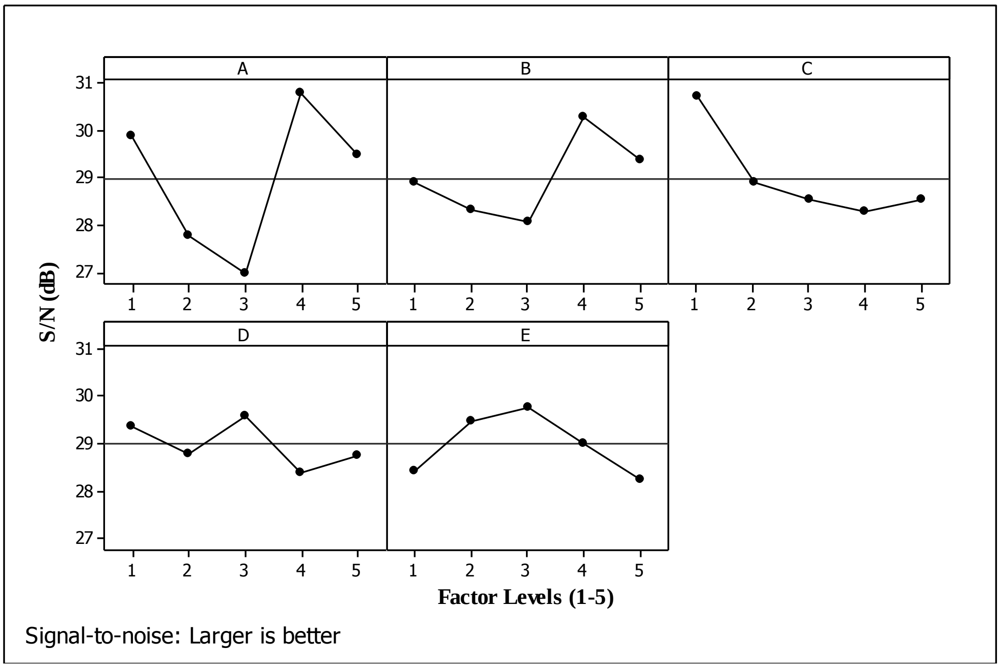

Figure 6. Main effects plot for S/N ratios

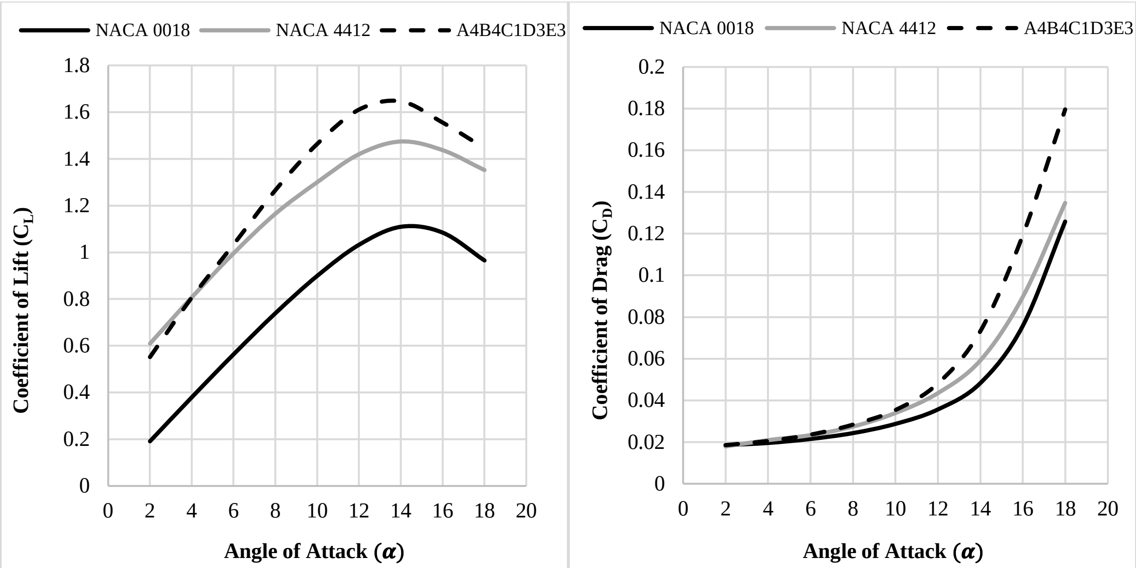

Figure 7. C_L and C_D values of the NACA 0018, NACA 4412 and the optimum design

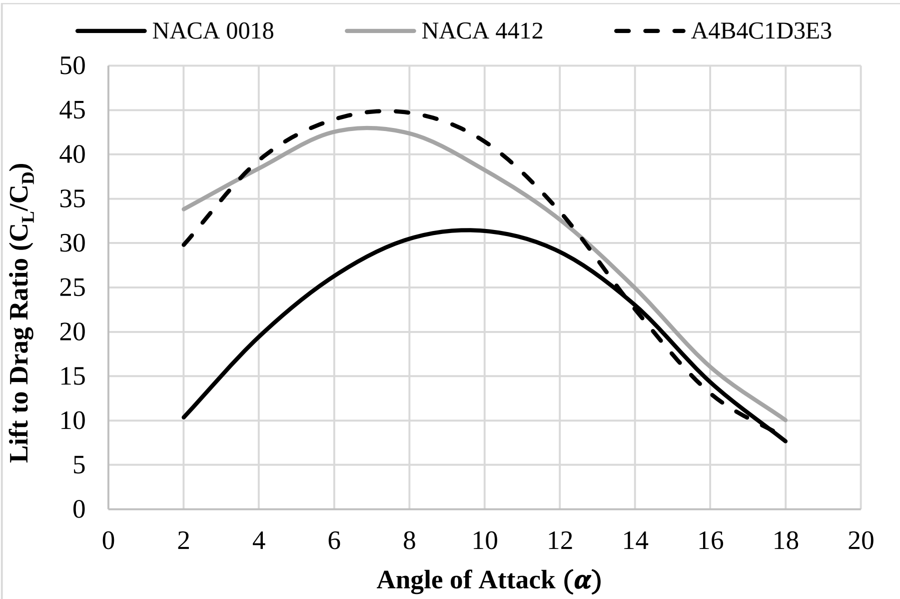

Figure 8. Comparison of Lift to Drag Ratios (C_L/C_D)